

Electronic Supplementary Information for:
**High energy density full lithium-ion cell based on specially
matched coulombic efficiency**

Bangkun Zou,^a Qiao Hu,^a Danqi Qu,^a Ran Yu,^a Yuting Zhou,^a Zhongfeng Tang,^a and
Chunhua Chen^{*a}

*a. CAS Key Laboratory of Materials for Energy Conversions, Department of
Materials Science and Engineering & Collaborative Innovation Center of Suzhou
Nano Science and Technology, University of Science and Technology of China,
Anhui Hefei 230026, China*

**E-mail: cchchen@ustc.edu.cn; Phone: +86-551-63606971; Fax: (+86)551-63601592.*

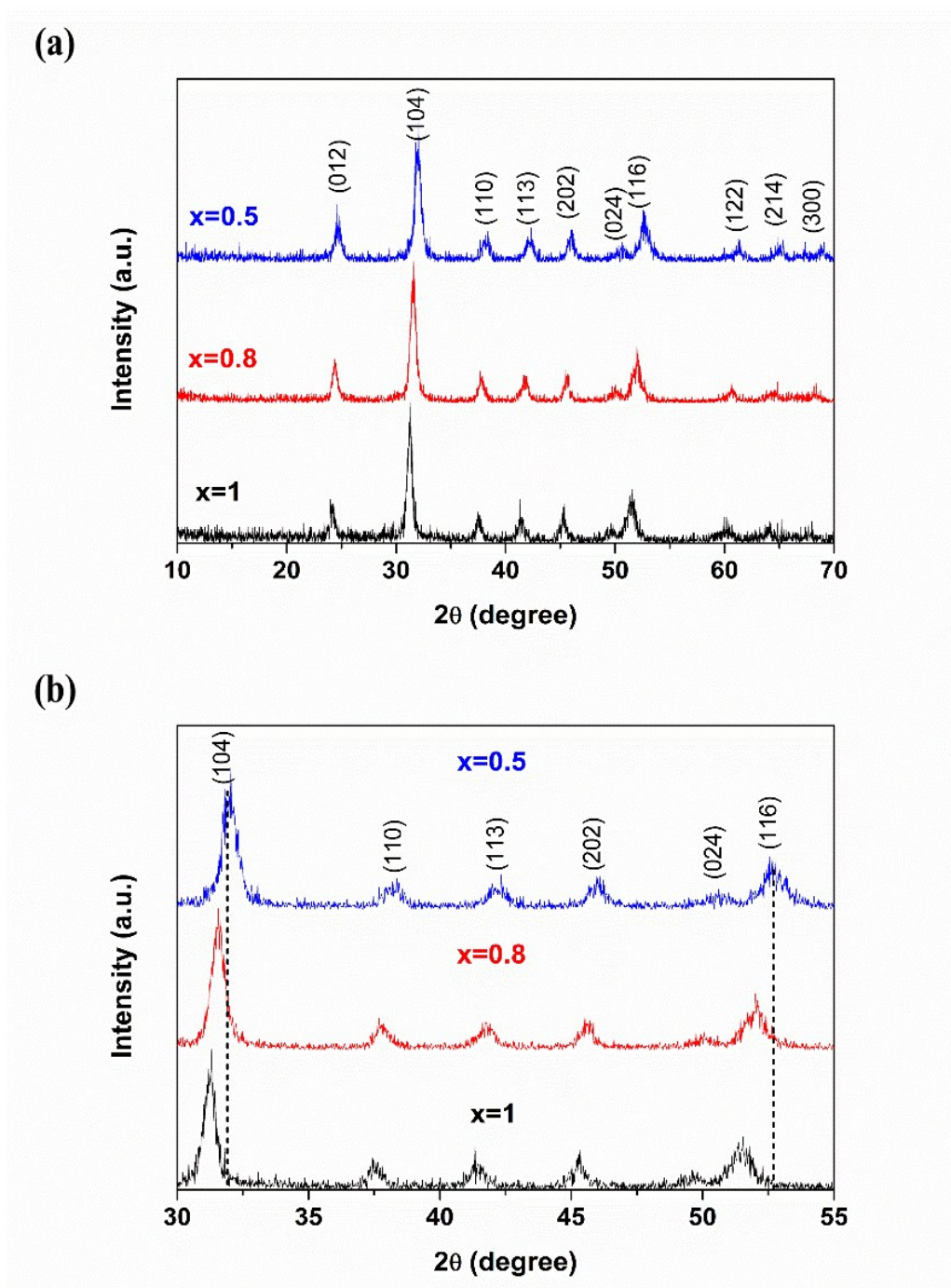


Fig. S1. XRD patterns of the as-solvothermal products $Mn_xCo_{1-x}CO_3$ ($x=1, 0.8, 0.5$), respectively (a). The diffraction patterns from 30° to 55° (2θ) are zoomed (b).

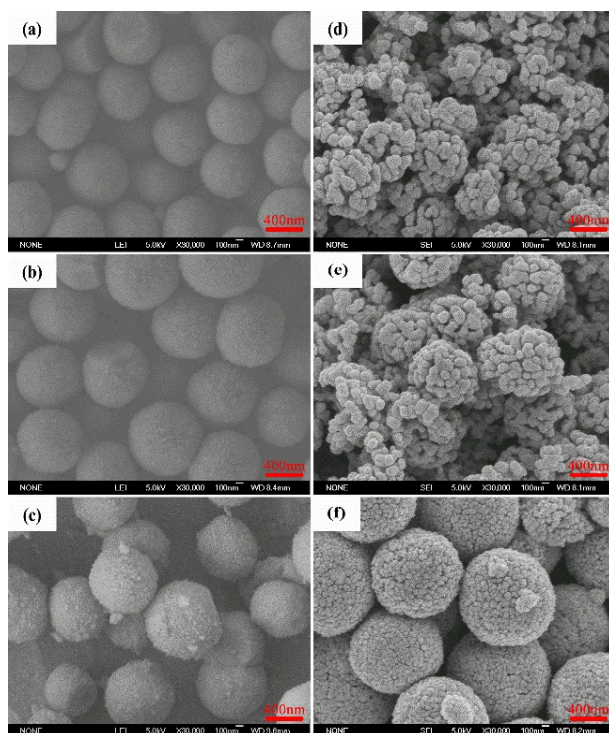


Fig. S2. SEM images of the $Mn_xCo_{1-x}CO_3$ precursors ($x=1, 0.8, 0.5$, a-c) and Mn_xCo_{1-x} oxides intermediates ($x=1, 0.8, 0.5$, d-f) after $600^\circ C$ calcination at air atmosphere.

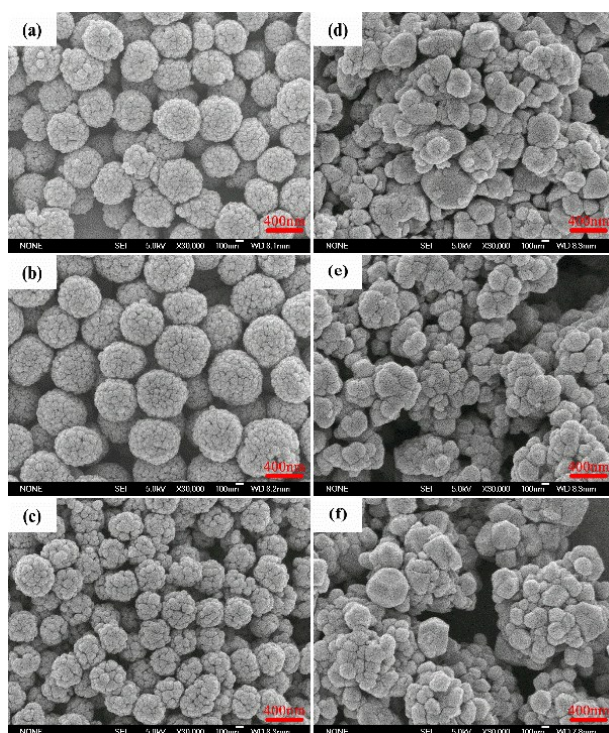


Fig. S3. SEM images of the $Mn_xCo_{1-x}O$ anodes ($x=1, 0.8, 0.5$, a-c), Li-rich cathodes with different compositions: LMNO (d), LMNCO (e) and LMCO (f).

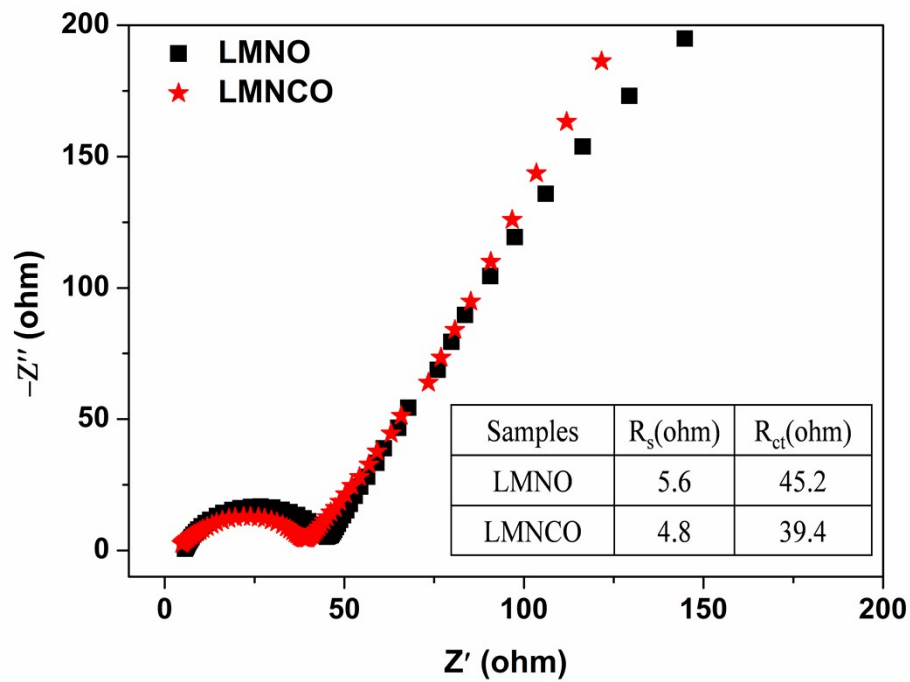


Fig. S4. The EIS of Li/LMNO (LMNCO) half-cells after 3 cycles at 0.1C. R_s represents the ohmic resistance and R_{ct} is the charge transfer resistance.

Table S1 The comparison of electrochemical performance of the Li-rich electrodes between this work and previously reported ones

Li rich materials	Cycling stability	Voltage stability	Refs
$\text{Li}_{1.2}\text{Mn}_{0.5}\text{Co}_{0.25}\text{Ni}_{0.05}\text{O}_2$	178.6 @0.8C (89.3%, 100 cycles)	--	1
Al_2O_3 coated $\text{Li}_{1.2}\text{Ni}_{0.2}\text{Mn}_{0.6}\text{O}_2$	192.9@0.2C (90.5%, 100 cycles)	--	2
Zr doped $\text{Li}_{1.2}\text{Mn}_{0.54}\text{Ni}_{0.13}\text{Co}_{0.13}\text{O}_2$	125@1C (78.6%, 100 cycles)	--	3
$\text{Li}_{1.231}\text{Mn}_{0.592}\text{Ni}_{0.2}\text{O}_2$	173.2@1C (89.73%, 69 cycles)	3.38 mV /cycle @0.1C	4
LiFePO_4 coated $\text{Li}_{1.2}\text{Mn}_{0.54}\text{Ni}_{0.13}\text{Co}_{0.13}\text{O}_2$	249.8@0.5C (92.8%, 120 cycles)	Negligible @0.5C	5
Cr doped $\text{Li}_{1.2}\text{Ni}_{0.2}\text{Mn}_{0.6}\text{O}_2$	200@0.08C (88.5%, 50 cycles)	≈ 2.8 mV /cycle @0.08C	6
$\text{Li}_{1.2}\text{Mn}_{0.54}\text{Ni}_{0.18}\text{Co}_{0.08}\text{O}_2$	216.5@0.8C (94.2%, 100 cycles)	1.4 mV /cycle @0.8C	7
$\text{Li}_{1.2}\text{Ni}_{0.2}\text{Mn}_{0.6}\text{O}_2$	141.3@1C (83.1%, 40 cycles)	--	8
Sn doped $\text{Li}_{1.2}\text{Ni}_{0.25}\text{Mn}_{0.55}\text{O}_2$	163@1.2C (92%, 200 cycles)	--	9
MgF_2 coated $\text{Li}_{1.2}\text{Ni}_{0.17}\text{Co}_{0.07}\text{Mn}_{0.56}\text{O}_2$	188@0.1C (86%, 50 cycles)	--	10
Na doped $\text{Li}_{1.14}\text{Ni}_{0.16}\text{Co}_{0.08}\text{Mn}_{0.57}\text{O}_2$	218.4@0.2C (98.8%, 100 cycles)	--	11
$\text{Li}_{1.2}\text{Ni}_{0.2}\text{Mn}_{0.6}\text{O}_2$	227.2@0.2C (95.8%, 130 cycles)	1.8 mV /cycle @0.2C	this work

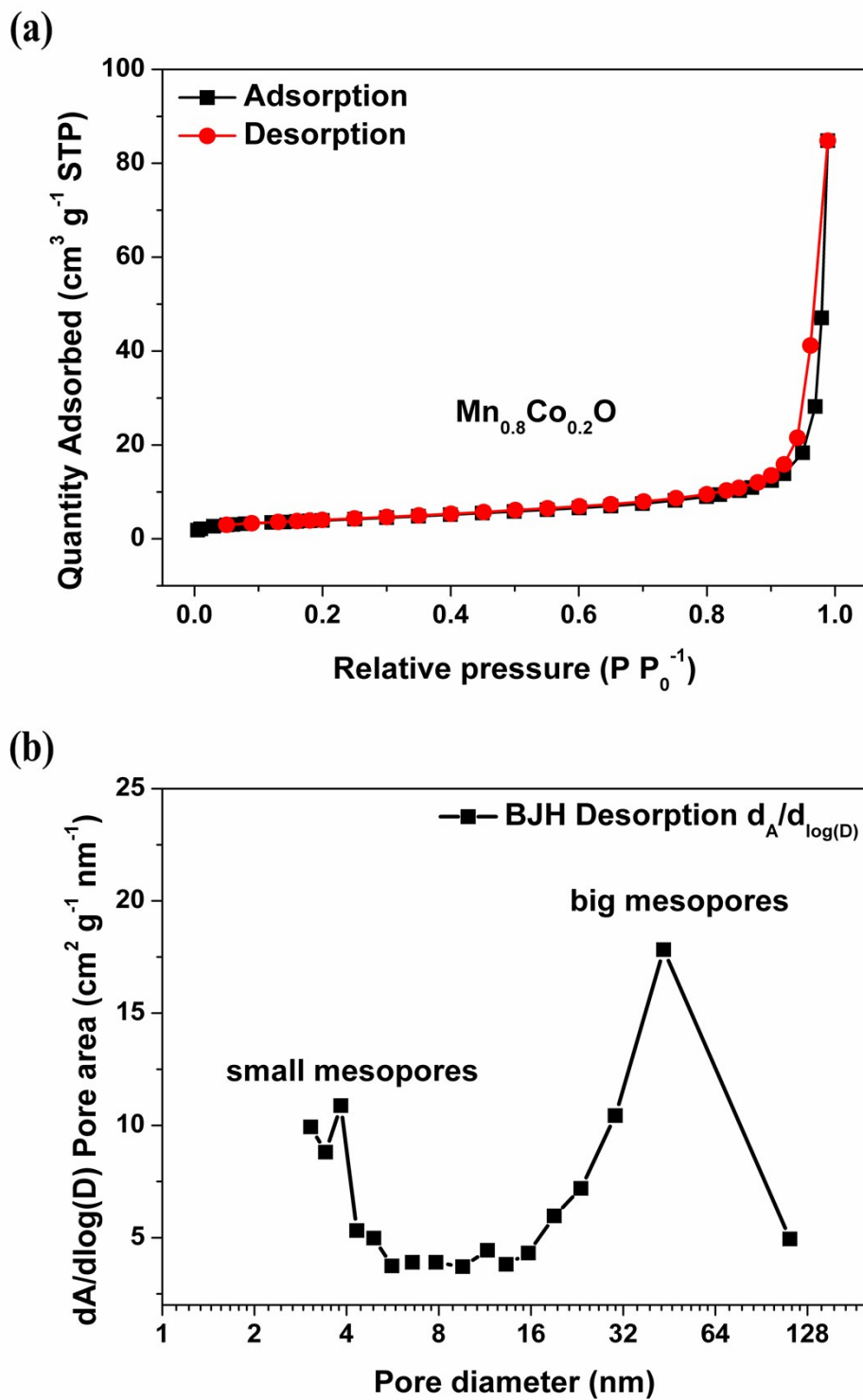


Fig. S5 The N_2 -adsorption/desorption curves (a), and pore size distribution (b) of $\text{Mn}_{0.8}\text{Co}_{0.2}\text{O}$ anode.

Table S2 The comparison of electrochemical performance of the MnO-based electrodes between this work and previously reported ones

MnO electrodes	Cycling stability	Rate stability	Refs
Carbon coated MnO	797.6 @0.1 A/g (112.1%, 50 cycles)	429.4 @0.8 A/g 323.2 @2 A/g	12
RGO coated MnO	1044.2 @0.1 A/g (90.8%, 120 cycles)	750 @0.8 A/g 600 @1.6 A/g	13
Carbon coated MnO	987.3 @0.1 A/g (80.9%, 150 cycles)	532.2 @1 A/g 406.1 @3 A/g	14
MnO/carbon nanotube composite	841 @0.1 A/g (93.4%, 200 cycles)	600 @0.76 A/g 400 @1.5 A/g	15
MnO@C/RGO	863 @0.38 A/g (119.7%, 160 cycles)	550 @3.8 A/g 415 @7.6 A/g	16
MnO yolk–shell sphere	1000 @0.2 A/g (107%, 500 cycles)	710 @2 A/g 513 @4 A/g	17
MnO@C	832 @0.1 A/g (120.6%, 100 cycles)	440 @1 A/g 315 @2 A/g	18
MnO/Graphene	930 @0.5 A/g (147.6%, 500 cycles)	500 @0.5 A/g 300 @1 A/g	19
Carbon coated and N-doped MnO	578 @0.1 A/g (95%, 60 cycles)	320 @0.5 A/g 187 @2 A/g	20
Hollow MnO	1050 @0.5 A/g (175%, 150 cycles)	770 @0.5 A/g 650 @1 A/g	21
MnO/C nanopeapods	510 @2 A/g (100%, 1000 cycles)	630 @1 A/g 470 @5 A/g	22
Mn _{0.8} Co _{0.2} O	682 @0.4 A/g (110%, 200 cycles)	583 @4 A/g 484 @8 A/g	this work

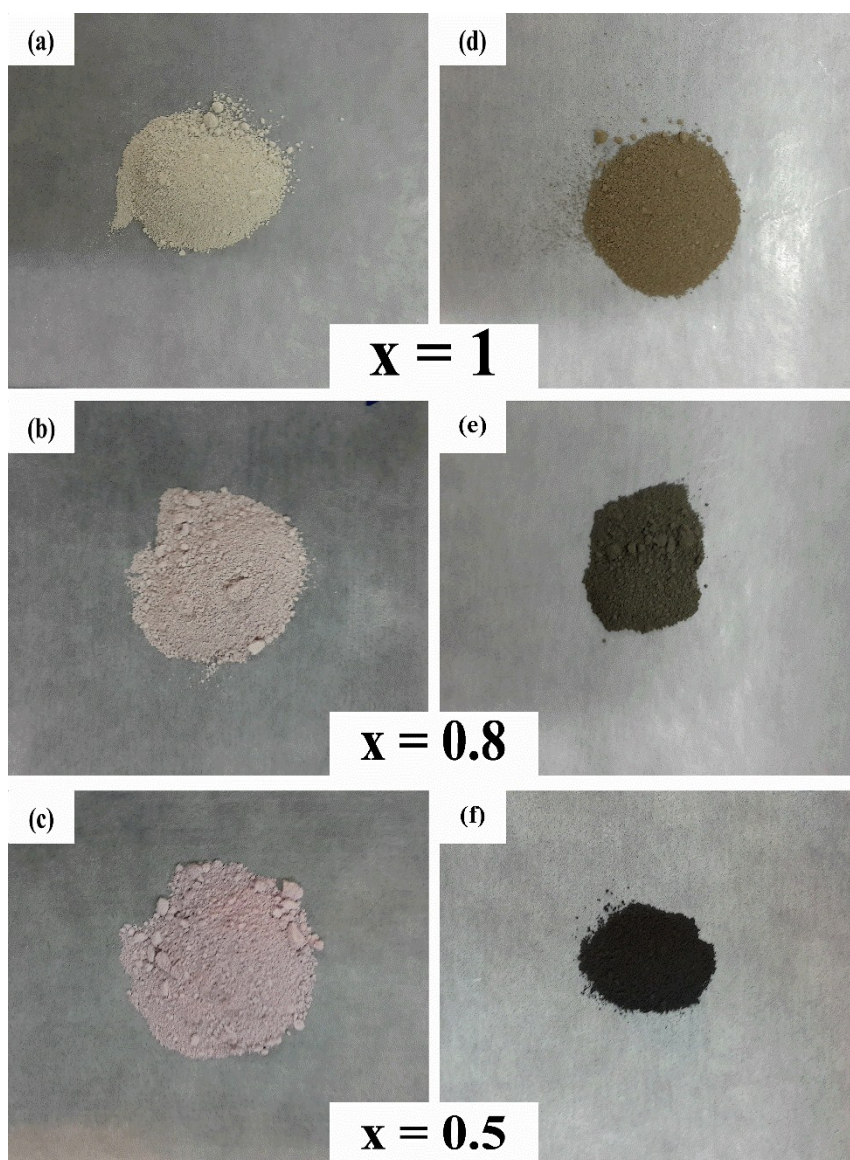


Fig. S6. The photos of the $\text{Mn}_x\text{Co}_{1-x}\text{CO}_3$ precursors ($x=1, 0.8, 0.5$, a-c) and the N_2 calcination products $\text{Mn}_x\text{Co}_{1-x}\text{O}$ anodes ($x=1, 0.8, 0.5$, d-f). The colors change from white to pink with the increase of Co content in the $\text{Mn}_x\text{Co}_{1-x}\text{CO}_3$ precursors, and the colors of the obtained $\text{Mn}_x\text{Co}_{1-x}\text{O}$ anodes change from brown to black in a way to provide that the electronic conductive of the anode materials is improved with increasing Co content.

Table S3 Comparison of electrodes' properties in assembling a full battery

Properties of electrodes	LMNO	Mn _{0.8} Co _{0.2} O	Graphite
Charge specific capacity (mAh g ⁻¹)	345	757	350
Discharge specific capacity (mAh g ⁻¹)	245	1040	372
Initial columbic efficiency	71.0%	72.8%	94.1%
Real density (g cm ⁻³)	≈2.50	5.45	2.25

References:

1. S. J. Shi, Z. R. Lou, T. F. Xia, X. L. Wang, C. D. Gu and J. P. Tu, *J. Power Sources*, 2014, **257**, 198-204.
2. L. L. Zhang, J. J. Chen, S. Cheng and H. F. Xiang, *Ceram. Int.*, 2016, **42**, 1870-1878.
3. Z. He, Z. Wang, H. Chen, Z. Huang, X. Li, H. Guo and R. Wang, *J. Power Sources*, 2015, **299**, 334-341.
4. Z. Zheng, S.-X. Liao, B.-B. Xu and B.-H. Zhong, *Ionics*, 2015, **21**, 3295-3300.
5. F. Zheng, C. Yang, X. Xiong, J. Xiong, R. Hu, Y. Chen and M. Liu, *Angew. Chem. Int. Ed.*, 2015, **54**, 13058-13062.
6. E. Lee, J. S. Park, T. P. Wu, C. J. Sun, H. Kim, P. C. Stair, J. Lu, D. H. Zhou and C. S. Johnson, *J. Mater. Chem. A*, 2015, **3**, 9915-9924.
7. Y. D. Zhang, Y. Li, X. Q. Niu, D. H. Wang, D. Zhou, X. L. Wang, C. D. Gu and J. P. Tu, *J. Mater. Chem. A*, 2015, **3**, 14291-14297.
8. Q. Zhang, J. Mei, X. Xie, X. Wang and J. Zhang, *Mater. Res. Bull.*, 2015, **70**, 397-402.
9. Q. Q. Qiao, L. Qin, G. R. Li, Y. L. Wang and X. P. Gao, *J. Mater. Chem. A*, 2015, **3**, 17627-17634.
10. S. Sun, N. Wan, Q. Wu, X. Zhang, D. Pan, Y. Bai and X. Lu, *Solid State Ionics*, 2015, **278**, 85-90.
11. F. Li, Y. Y. Sun, Z. H. Yao, J. S. Cao, Y. L. Wang and S. H. Ye, *Electrochim. Acta*, 2015, **182**, 723-732.

12. J. Liu, N. Chen and Q. Pan, *J. Power Sources*, 2015, **299**, 265-272.
13. G. Xu, F. Jiang, Z.-a. Ren and L.-w. Yang, *Ceram. Int.* 2015, 41, 10680-10688.
14. X. Zhao, Y. Du, L. Jin, Y. Yang, S. Wu, W. Li, Y. Yu, Y. Zhu and Q. Zhang, *Sci. rep.*, 2015, **5**, 14146.
15. X. Cui, Y. Wang, Z. Chen, H. Zhou, Q. Xu, P. Sun, J. Zhou, L. Xia, Y. Sun and Y. Lu, *Electrochim Acta*, 2015, **180**, 858-865.
16. D. H. Liu, H. Y. Lu, X. L. Wu, B. H. Hou, F. Wan, S. D. Bao, Q. Y. Yan, H. M. Xie and R. S. Wang, *J. Mater. Chem. A*, 2015, **3**, 19738-19746.
17. S. B. Wang, C. L. Xiao, Y. L. Xing, H. Z. Xu and S. C. Zhang, *J. Mater. Chem. A*, 2015, **3**, 15591-15597.
18. J. G. Wang, C. B. Zhang, D. D. Jin, K. Y. Xie and B. Q. Wei, *J. Mater. Chem. A*, 2015, **3**, 13699-13705.
19. S. Zhang, L. Zhu, H. Song, X. Chen and J. Zhou, *Nano Energy*, 2014, **10**, 172-180.
20. H. Liu, Z. Li, Y. Liang, R. Fu and D. Wu, *Carbon*, 2015, **84**, 419-425.
21. J. Yue, X. Gu, L. Chen, N. N. Wang, X. L. Jiang, H. Y. Xu, J. Yang and Y. T. Qian, *J. Mater. Chem. A*, 2014, **2**, 17421-17426.
22. H. Jiang, Y. J. Hu, S. J. Guo, C. Y. Yan, P. S. Lee and C. Z. Li, *Acs Nano*, 2014, **8**, 6038-6046.